International Journal of Modern Physics E
Vol. 14, No. 3 (2005) 395–402

World Scientific
www.worldscientific.com

SKYRME–HARTREE–FOCK CALCULATIONS OF FISSION BARRIERS OF THE HEAVIEST AND SUPERHEAVY NUCLEI

ANDRZEJ STASZCZAK[*,†,‡], JACEK DOBACZEWSKI[§,†,‡,¶],
WITOLD NAZAREWICZ[†,‡,§,‖]

[*] *Institute of Physics, Maria Curie-Skłodowska University, pl. M. Curie-Skłodowskiej 1, 20-031 Lublin, Poland*
[†] *Department of Physics and Astronomy, University of Tennessee, Knoxville, TN 37996, USA*
[‡] *Physics Division, Oak Ridge National Laboratory, P.O. Box 2008, Oak Ridge, TN 37831, USA*
[§] *Institute of Theoretical Physics, Warsaw University, ul. Hoża 69, 00-681 Warsaw, Poland*
[¶] *Joint Institute for Heavy Ion Research, Oak Ridge, TN 37831, USA*
[*] *stas@tytan.umcs.lublin.pl*
[¶] *jacek.dobaczewski@fuw.edu.pl*
[‖] *witek@utk.edu*

Received 24 September 2004
Revised 17 November 2004

Self-consistent Skyrme–Hartree–Fock (SHF) calculations of static fission barriers are presented for even-even Fermium isotopes as well as for superheavy even-even N=184 isotones. In the particle-hole channel, we use the SLy4 Skyrme parametrization, while in the particle-particle channel we take a T=1 seniority pairing force treated in the BCS approximation. The influence of reflection-asymmetric and triaxial degrees of freedom on the static fission paths are investigated.

1. Introduction

Nuclear fission is one of the best examples of the nuclear large-amplitude collective motion. Microscopically, fission can be viewed as a many-body tunneling through a potential barrier, which is difficult to treat if one wants to go beyond the standard semiclassical approximation.[1,2,3] Various nuclear structure models (including a microscopic-macroscopic approach and self-consistent approaches both nonrelativistic and relativistic) have been applied to the fission barriers, lifetimes, and mass/charge distributions, and a large sensitivity to model details and parametrizations has been found.[4] (For a recent review of self-consistent mean-field models and parametrizations, see Bender *et al.*[5])

Recently, a number of theoretical calculations of the static fission barriers of nuclei in the actinide and trans-actinide regions have been carried out. These include calculations based on the microscopic-macroscopic treatment,[6] the self-consistent approach with the Gogny[7] and Skyrme[8,9] forces, and also within the relativistic mean field model.[9]

The aim of this contribution is to calculate static fission barriers for the even-even Fermium isotopes and the even-even superheavy nuclei with N=184 using the energy density functional with the Skyrme interaction SLy4[10] and a seniority pairing force treated in the BCS approximation. The calculations were carried out using the Hartree-Fock+BCS code HFODD (v.2.8i) that solves the self-consistent HF equations by using a Cartesian (3D) harmonic oscillator (HO) finite basis.[11] This code makes it possible to break all self-consistent symmetries of the nuclear mean field, including axial symmetry, reflection symmetry, and time reversal. Particular attention has been paid to symmetry-breaking effects along the fission path. The pairing strengths have been adjusted to reproduce the proton and neutron experimental pairing gaps in ^{252}Fm.

2. Results

First, we have studied the stability of our results with respect to the number of the deformed HO states ($N_{\rm limit}$) used in this basis. Figure 1 shows the calculated self-consistent potential energy curve of ^{240}Pu as a function of the axial quadrupole

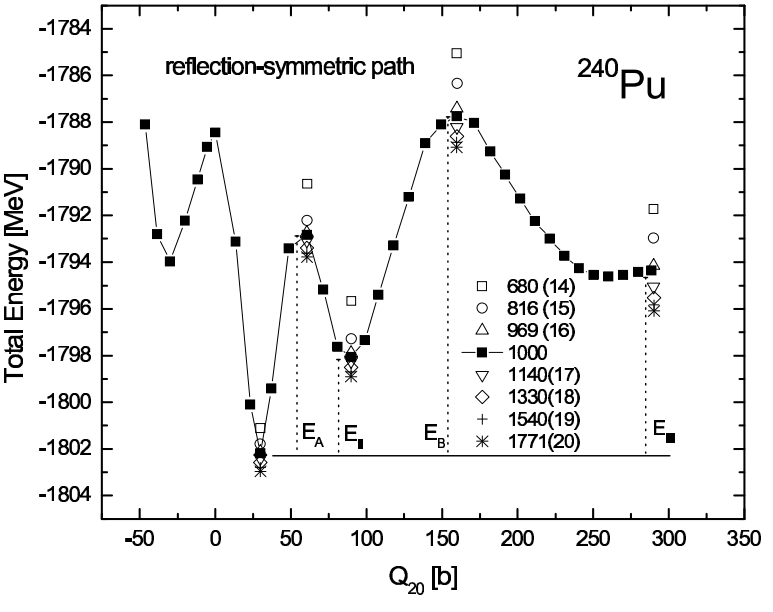

Fig. 1. Stability of the calculated SHF+BCS energy curve for ^{240}Pu as a function of the harmonic-oscillator basis size, see text.

constraint $Q_{20} = \langle \hat{Q}_{20} \rangle$. The solid line corresponds to $N_{\rm limit}$=1000 deformed HO states included in the basis. At each value of Q_{20}, the HO basis deformation is determined as that corresponding to Q_{20} through the standard first-order expression.[11] Therefore, the set of HO states included in the basis changes with the changing nuclear shape. The results with different values of $N_{\rm limit}$=680 (14 spherical oscillator shells included at Q_{20}=0), 816 (15), 969 (16), 1140 (17), 1330 (18), 1540 (19), and 1771 (20) are also shown at the extreme points (minima and maxima) of the potential energy curve. It is seen that the rate of convergence weakly depends on the quadrupole deformation, and for larger elongations is slightly slower than at sphericity. As shown in Fig. 1, reliable calculations can be carried out with $N_{\rm limit}$ = 1140 (17), and the errors related to the finite basis sizes that impact energies of the first (E_A) and second (E_B) barrier are less than 1 MeV.

Having determined the basis size, we performed the set of calculations for the series of even-even Fermium isotopes which are experimentally known to exhibit rapid variations of the spontaneous fission half-lives. Two fission paths corresponding to bimodal fission have been investigated. The usual reflection-asymmetric path corresponds to two fission fragments with different masses. The reflection-symmetric path can be associated with division into symmetric, nearly spherical fragments with high kinetic energies. In our calculations, the quadrupole and octupole mass moments were used as constraints. The non-zero octupole mass moment Q_{30} indicates the breaking of intrinsic parity, while the presence of the quadrupole moment Q_{22} signals the appearance of triaxial distortions.

Deformation energy curves ($E^{\rm tot}$) and the mass octupole moments (Q_{30}) calculated along static fission paths for the even-even Fermium isotopes with the neutron numbers N=142–164 are plotted in Figs. 2 and 3 as functions of the mass quadrupole moment Q_{20}. All calculated static barriers have similar, two-humped shapes. The sizes of the static fission barriers are correlated with the experimentally known increase in the spontaneous fission half-lives for the lighter Fermium isotopes with N=142-152. The influence of triaxial asymmetry on the height of the first fission barrier is shown as a difference between the open and solid symbols. The effect of triaxiality increases with neutron number and reaches about 3 MeV for $N \geq 150$. For $Q_{20} < 130$ b, the fission paths of nuclei displayed in Fig. 2 exhibit reflection-symmetric shapes ($Q_{30} = 0$), while the reflection-asymmetric paths ($Q_{30} \neq 0$) takes over at larger elongations with $Q_{20} > 130$ b. For the heavier Fm isotopes displayed in Fig. 3, the transition to the reflection-asymmetric path occurs at greater values of Q_{20} and the transition point increases with N. In the extreme case of ^{264}Fm (which is expected to fission into two doubly magic ^{132}Sn nuclei), the fission path becomes reflection-symmetric. The disappearance of the reflection-asymmetric path at large neutron numbers gives rise to the reduction, or even disappearance, of the second fission barrier. This reduction plays a crucial role in the standard interpretation of the experimentally known rapid decrease of the spontaneous fission half-lives in the heavy Fm isotopes.

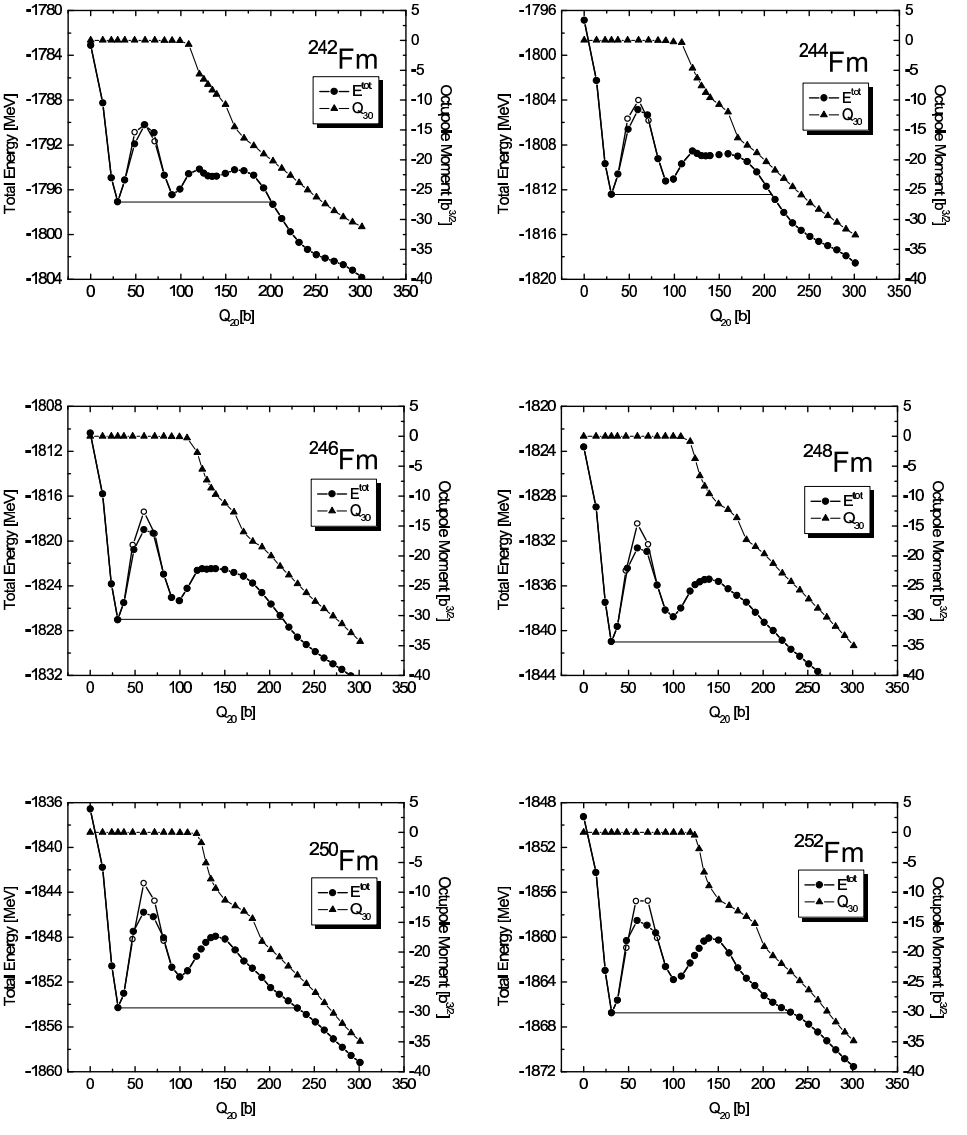

Fig. 2. Total binding energy $E^{\rm tot}(\bullet)$ and the mass octupole moments $Q_{30}(\blacktriangle)$ calculated along the lowest static fission paths for the even-even Fermium isotopes with N=142–152. The differences between the open and solid symbols in the region of the first barrier represent the energy gain due to triaxiality. $N_{\rm limit}$=1140 was used.

In order to better understand the competition between reflection-symmetric and reflection-asymmetric fission valleys, we show in Fig. 4 the total energy curves for $^{254-264}$Fm calculated with a smaller basis $N_{\rm limit}$=680. For each nucleus the two different fission paths are displayed: reflection-asymmetric (open symbols) and reflection-symmetric (solid symbols). It is seen that at large values of Q_{20}, the bar-

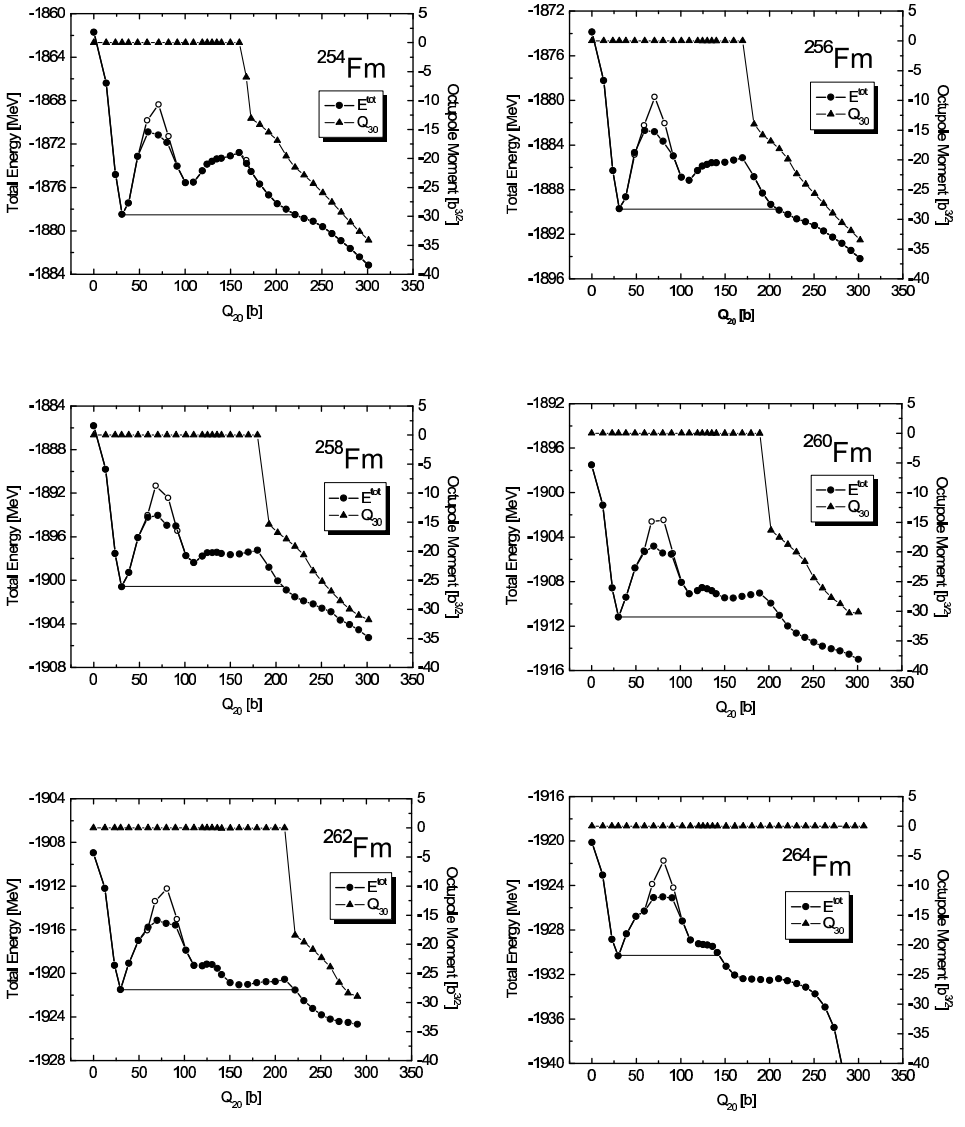

Fig. 3. Similar as in Fig. 2 except for the even-even Fermium isotopes with N=154-164.

riers along the reflection-asymmetric paths are more narrow, whereas the distinctly higher second humps appear.

Figure 5 shows the deformation energy curves and the mass hexadecapole moments calculated along the static fission paths of the superheavy even-even nuclei with N=184 (which is the neutron magic gap in this region.[12]) These results markedly differ from those obtained for the Fm isotopes. As expected,[12] all N=184 isotones have spherical ground states. The corresponding static two-humped fission barriers are narrow and reflection-symmetric. The triaxial deformation lowers the

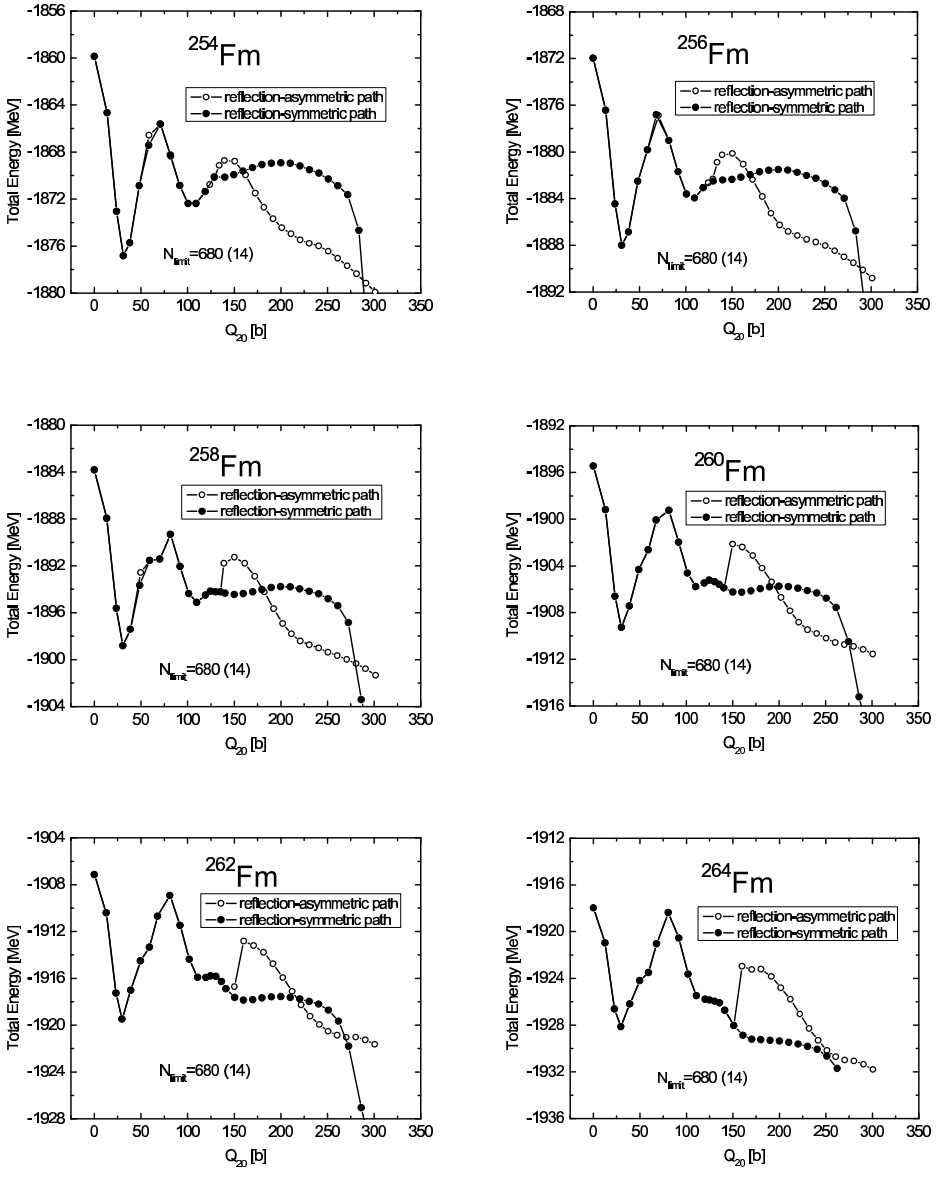

Fig. 4. Total binding energy $E^{\rm tot}$ calculated along the static fission path for the even-even Fermium isotopes $^{254-264}$Fm. Open (closed) symbols represent the reflection-asymmetric (symmetric) path. As compared to Figs. 2 and 3, the size of the oscillator basis is slightly reduced, $N_{\rm limit}$=680.

first barrier, with the maximum reduction (2 MeV) predicted for ^{308}124. As illustrated in Fig. 5, with increasing Z, the height of the first barrier increases while the second barrier gets reduced. The increase in the hexadecapole moment along the fission path reflects the development of the neck.

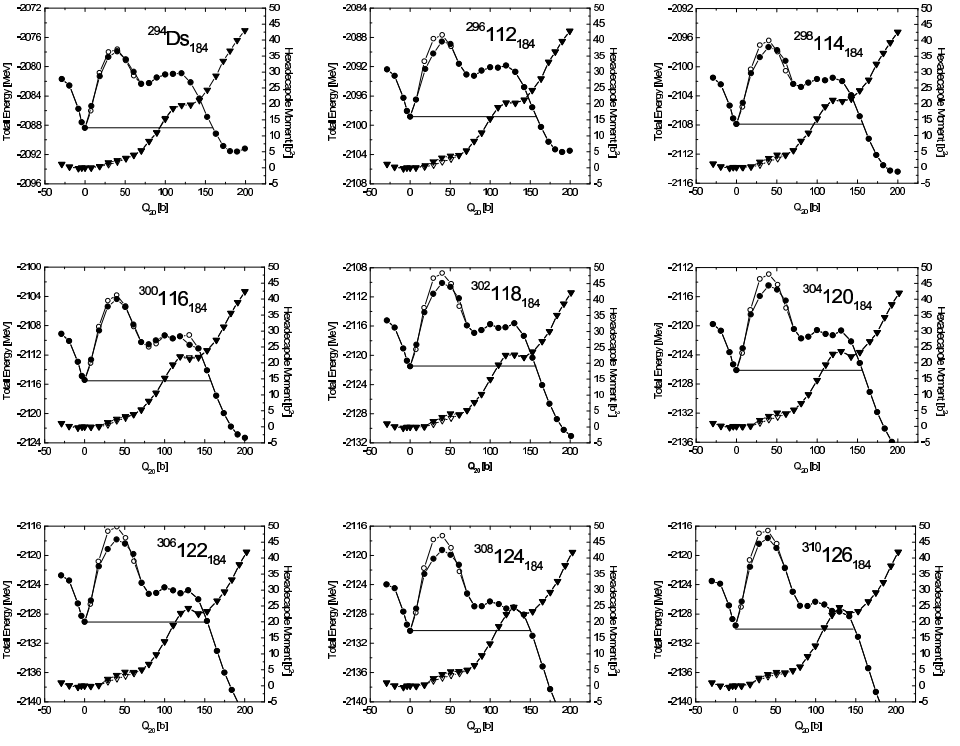

Fig. 5. Total binding energy $E^{\rm tot}(\bullet)$ and the mass hexadecapole moment $Q_{40}(\blacktriangledown)$ as a function of Q_{20} for the even-even superheavy nuclei with $N = 184$. The differences between the open and solid symbols represent the effect of triaxiality on the first barrier.

3. Conclusion

We have applied the SHF+BCS method with the Skyrme parametrization SLy4 to study static fission barriers of the even-even Fm isotopes and the superheavy isotones of N=184. The overall qualitative agreement with existing experimental data for Fm isotopes is satisfactory. In particular, our SHF calculations explain the spectacular non-linear behavior of the observed spontaneous fission half-lives of the Fm isotopes. Further dynamical calculations are planned to pin down the competition between alpha decay and spontaneous fission in the heaviest and superheavy nuclei.

Acknowledgments

This work was supported in part by the National Nuclear Security Administration under the Stewardship Science Academic Alliances program through the U.S. Department of Energy Research Grant DE-FG03-03NA00083; by the U.S. Department of Energy under Contract Nos. DE-FG02-96ER40963 (University of Tennessee), DE-AC05-00OR22725 with UT-Battelle, LLC (Oak Ridge National Laboratory),

and DE-FG05-87ER40361 (Joint Institute for Heavy Ion Research); by the Polish Committee for Scientific Research (KBN) under Contract No. 1 P03B 059 27; and by the Foundation for Polish Science (FNP).

References

1. J. W. Negele, *Nucl. Phys.* **A502** (1989) 371c.
2. W. Nazarewicz, *Nucl. Phys.* **A557** (1993) 489c.
3. A. Bonasera and A. Iwamoto, *Phys. Rev. Lett.* **78** (1997) 121.
4. M. Bender, K. Rutz, P. G. Reinhard and J. A. Maruhn, *Eur. Phys. J.* **A7** (2000) 467.
5. M. Bender, P.-H. Heenen and P.-G. Reinhard, *Rev. Mod. Phys.* **75** (2003) 121.
6. A. Baran, Z. Łojewski and K. Sieja, *Int. J. Mod. Phys.* **E13** (2004) 353.
7. M. Warda, J. L. Egido, L. M. Robledo and K. Pomorski, *Phys. Rev.* **C66** (2002) 014310.
8. L. Bonneau, P. Quentin and D. Samsœn, *Eur. Phys. J.* **A21** (2004) 391.
9. T. Bürvenich, M. Bender, J. A. Maruhn and P.-G. Reinhard, *Phys. Rev.* **C69** (2004) 014307.
10. E. Chabanat, P. Bonche, P. Haensel, J. Meyer and F. Schaeffer, *Nucl. Phys.* **A635** (1998) 231.
11. J. Dobaczewski and J. Dudek, *Comput. Phys. Commun.* **102** (1997) 166; **102** (1997) 183; **131** (2000) 164; J. Dobaczewski and P. Olbratowski, *ibid.* **158** (2004) 158.
12. S. Ćwiok, J. Dobaczewski, P.-H. Heenen, P. Magierski and W. Nazarewicz, *Nucl. Phys.* **A611** (1996) 211.